

Exclusive Signals of an Extended Higgs Sector

Nathaniel Craig,^{a,b} Scott Thomas^a

^a*Department of Physics, Rutgers University
Piscataway, NJ 08854*

^b*School of Natural Sciences, Institute for Advanced Study
Princeton, NJ 08540*

ABSTRACT: Expectations for the magnitude of Higgs boson signals in standard Higgs search channels at the LHC relative to Standard Model (SM) expectations are investigated within the framework of various types of CP and flavor conserving two Higgs doublet models (2HDMs). Signals of the SM-like Higgs boson in different classes of 2HDM may be parameterized in terms of particular two-dimensional sub-spaces of the general four-dimensional space of Higgs couplings to the massive vector bosons, top quark, bottom quark, and tau lepton. We find fairly strong correlations among the inclusive di-photon channel and the exclusive di-photon and di-tau channels from vector boson fusion or associated production. Order one deviations from SM expectations in some of these channels could provide discriminating power among various types of 2HDMs. The ratio of exclusive di-photon to di-tau channels is particularly sensitive to deviations from SM expectations. We also emphasize that deviations from SM expectations in standard Higgs search channels may imply observable signals of non-SM-like Higgs bosons in some of these same channels, in particular in di-photon and di-vector boson channels. The results cataloged here provide a roadmap for interpreting standard Higgs search channels in the context of 2HDMs.

Contents

| | | |
|----------|---|-----------|
| 1 | Introduction | 1 |
| 2 | Standard Higgs channels | 3 |
| 3 | Extended Higgs sectors | 4 |
| 4 | SM-like Higgs inclusive production | 7 |
| 4.1 | Inclusive di-photon | 9 |
| 4.2 | Inclusive VV^* | 9 |
| 4.3 | Inclusive ratios | 9 |
| 5 | SM-like Higgs exclusive production | 11 |
| 5.1 | Exclusive VBF/ Wh/Zh di-photon | 11 |
| 5.2 | Exclusive VBF/ Wh/Zh VV^* | 14 |
| 5.3 | Exclusive VBF $\tau\tau$ | 14 |
| 5.4 | Exclusive VBF/ Wh $b\bar{b}$ | 15 |
| 5.5 | Exclusive $t\bar{t}h$ di-photon | 16 |
| 5.6 | Exclusive ratios | 17 |
| 6 | Heavy non-SM-like scalars | 18 |
| 7 | Conclusion | 21 |

1 Introduction

The Large Hadron Collider (LHC) is poised to reveal the mechanism of electroweak symmetry breaking. Recent results from ATLAS and CMS exclude a light Standard Model Higgs boson for all but a narrow mass range, with intriguing hints of a possible excess in the vicinity of 125 GeV [1, 2]. If a light scalar is discovered at the LHC in conventional Higgs search channels, the immediate question will be whether its properties are those of the Standard Model Higgs boson. This question will begin to be probed in several ways with a relatively low amount of integrated luminosity, both by measuring cross section times branching ratios in standard Higgs search channels, and by possibly observing additional degrees of freedom in these or other channels. Unsurprisingly, considerable effort has recently been devoted to studying the potential implications of standard search channels for probing the couplings of a Higgs near 125 GeV [3] and the prospects for measuring couplings with additional integrated luminosity [4, 5].¹

Although it is possible to envision special-purpose measurements aimed specifically at measuring the couplings of a Standard Model-like (SM-like) Higgs boson, or new searches aimed at discovering

¹Sharper questions, such as whether the vertex structure of the coupling between the Higgs and gauge bosons corresponds to that expected from electroweak symmetry breaking, may also be answerable with greater integrated luminosity [6].

additional states, a great deal may be learned simply by studying the effects of non-standard Higgs properties on ongoing searches in the standard Higgs search channels. At present, considerable experimental effort has been devoted to these standard Higgs search channels – i.e., the ones most promising for observing production and decay of the Standard Model Higgs boson. The dominant production mode in this case is through gluon-gluon fusion (ggF), $gg \rightarrow h$, which benefits from a large cross section and the resonant production of the Higgs. But there are also a variety of ancillary channels in which the Higgs is produced in association with other quarks or vector bosons; these channels typically have smaller backgrounds due to the availability of additional reconstructable objects in the final state. These are, in order of decreasing production rate: weak vector boson fusion (VBF), $qq \rightarrow qqh$; Vh associated production, $q\bar{q}' \rightarrow Wh, Zh$; and $t\bar{t}h$ associated production, $q\bar{q}, gg \rightarrow t\bar{t}h$. For a given Higgs final state, it is possible to measure both *inclusive* production, in which all production channels are combined; and *exclusive* production, in which the distinctive properties of certain associated production channels may be isolated. While the former offers the largest possible signal, the latter offers lower backgrounds and the possibility of distinguishing the magnitude of various Higgs couplings.

On the decay side, the final states with the greatest discovery potential are $h \rightarrow \gamma\gamma$, $h \rightarrow ZZ^* \rightarrow 4\ell$, and $h \rightarrow WW^* \rightarrow \ell\ell\nu\nu$. The distinctive final state topology of the di-photon channel makes it a crucial search channel for lighter masses despite the relatively small signal. Similarly, the cleanliness of the 2ℓ and 4ℓ final states from WW^* and ZZ^* production make $h \rightarrow \ell\ell\nu\nu$ and $h \rightarrow 4\ell$ particularly attractive. The $h \rightarrow \tau\tau$ and $h \rightarrow b\bar{b}$ final states are also fairly promising due to the potentially large branching ratios, though the size of QCD backgrounds to these processes means that they are plausibly observable only in associated production channels, where the additional tagging information helps to improve the signal-to-background ratio. A final possibility is to probe the various non-resonant multilepton final states available through both gluon-gluon fusion and various associated production modes [7]. While this approach does not offer sharp mass resolution, the low backgrounds to many nonresonant same-sign two-, three- and four-lepton Higgs final states provides considerable sensitivity.

To the extent that searches in many of these standard Higgs channels are underway, it is worth examining how they may probe for deviations from a Standard Model Higgs sector. Since the production and decay rates of the Standard Model Higgs are completely determined in terms of its mass, it is possible to compare cross section times branching ratio signals in standard Higgs channels to the SM expectation, and thereby obtain information about the relative strength of the couplings of a SM-like Higgs boson. In this respect, exclusive standard channels are particularly useful. The background to many exclusive channels is low, putting a variety of channels within reach at low luminosity. Different exclusive production channels depend on different Higgs couplings, and therefore may be used to separately probe Higgs couplings to fermions and gauge bosons. Perhaps most attractively, it is possible to measure the ratios of various exclusive channels, in which case many systematic errors drop out and functions of ratios of couplings may be measured with the greatest possible accuracy. Needless to say, these channels may also be sensitive to additional states in the Higgs sector and can play a further role in their discovery and characterization.

In this work we examine the range of signals appearing in standard Higgs search channels in minimal extensions of the electroweak symmetry breaking sector. We focus on perhaps the simplest class of extended electroweak symmetry breaking: theories with an additional Higgs doublet. Such two Higgs doublet models (2HDM) are well-motivated on their own by beyond-the-Standard-Model theories such as supersymmetry, and also serve as comprehensive effective theories for more exotic means of electroweak symmetry breaking. As simple effective theories for extended EWSB, 2HDM have attracted considerable attention with regard to Higgs searches at the LHC; for recent related work on 2HDM signals see e.g. [8].

We focus on standard Higgs search channels that should be accessible with a relatively low amount of integrated luminosity, roughly $\mathcal{O}(30 - 50) \text{ fb}^{-1}$ at each LHC experiment; this amounts to data adequate for Standard Model Higgs discovery as well as observation of various exclusive production and decay channels. We neglect other channels that are more model-dependent, including additional non-Standard Model decays among the various scalars of a 2HDM. For the sake of definiteness, we will assume when necessary that the mass of the SM-like Higgs boson, h , is $m_h = 125 \text{ GeV}$, with other scalars heavier. Our focus lies on two particularly interesting phenomena: (1) the range and correlation of (ratios of) cross section times branching ratio measurements for the SM-like Higgs boson in both inclusive and exclusive channels that can be realized in various 2HDM; and (2) the relation between potential discrepancies in these measurements and the contribution of additional Higgs bosons to standard Higgs search channels. Our purpose is not to quantify the precision with which measurements may be performed in various channels, but rather to explore possible ranges for (sizable) deviations from Standard Model Higgs predictions that could arise in a post discovery-level data set. In this sense we provide a road map for the interpretation of any deviations that might arise in early observations of both inclusive and exclusive channels within the framework of two Higgs doublets.

To this end, in Section 2 we enumerate the various inclusive and exclusive standard Higgs channels that should be observable with relatively low integrated luminosity. In Section 3 we review the structure of the simplest 2HDMs and their couplings to Standard Model fermions and gauge bosons. In Section 4 we consider the ranges of various (ratios of) inclusive cross section time branchings of the SM-like Higgs h in various 2HDMs. We then turn in Section 5 to consider (ratios of) exclusive cross section times branching ratios of the SM-like Higgs h , as well as correlations among various exclusive channels. In Section 6 we turn our attention to the other non-SM-like scalars in 2HDMs. We show that within 2HDMs, discrepancies of certain cross section times branching ratios for the SM-like Higgs can imply that some of the heavier scalars may be observed in standard Higgs search channels. We discuss conclusions and future directions in Section 7.

2 Standard Higgs channels

As discussed in the introduction, there are a number of standard channels, both inclusive and exclusive, that should be observable with relatively low integrated luminosity after the discovery of a SM-like Higgs boson. The exclusive channels potentially available in the early post-discovery data set are particularly attractive. Although the cross sections for exclusive channels are considerably smaller than their inclusive counterparts, the backgrounds are typically lower. The ability to isolate a particular production process makes these exclusive channels particularly useful, as does the possibility of measuring exclusive ratios, for which many systematics drop out. In this sense, exclusive ratios may provide the first sensitive probe of Higgs couplings.

To be more specific, in Table 1 we list the standard Higgs channels we estimate to be potentially observable in the early data set, assuming Standard Model cross sections for a Higgs mass of $m_h = 125 \text{ GeV}$. The di-photon final state is the most promising, and should be observable in every production channel. The $t\bar{t}h$ di-photon signal is very small, but nonetheless should be observable above the (relatively low) background. The $h \rightarrow WW^* \rightarrow 2\ell 2\nu$ final state should be observable in both inclusive production and separately in VBF. It is also possible that the leptonic WW decays will be accessible in Vh and potentially $t\bar{t}h$ associated production through the nonresonant multi-lepton final states. Similarly, $h \rightarrow ZZ^* \rightarrow 4\ell$ should be separately visible in both inclusive production and VBF. The prospects for observing leptonic $h \rightarrow ZZ^*$ decays in Vh and $t\bar{t}h$ are somewhat poor, due to the large

Standard Model background for multi-lepton final states involving two or more Z bosons. The decay $h \rightarrow \tau\tau$ should be visible in the exclusive VBF channel when one or both τ 's decay leptonically; backgrounds for $h \rightarrow \tau\tau$ produced in gluon fusion are prohibitively high, while the production cross sections for other associated channels are low. Finally, the purely hadronic decay $h \rightarrow \tau\tau$ should be observable in the Vh and VBF associated production channels. Note that results for LHC searches in some of these channels are available with 5 fb^{-1} at 7 TeV, including $h \rightarrow \gamma\gamma$ (both inclusive and VBF) [9, 10]; $h \rightarrow ZZ^* \rightarrow 4\ell$ inclusive [11, 12]; $h \rightarrow WW^* \rightarrow 2\ell 2\nu$ inclusive [13]; $h \rightarrow \tau\tau$ in VBF [14]; and $h \rightarrow b\bar{b}$ in Vh associated production [15].

Table 1. Higgs search channels that are potentially observable with relatively low integrated luminosity post-discovery of a light SM-like Higgs boson. Gray checks ($t\bar{t}h$ with $h \rightarrow \gamma\gamma$ or $h \rightarrow WW^*$; Vh with $h \rightarrow WW^*$; VBF with $h \rightarrow b\bar{b}$) denote borderline channels that may be more challenging to observe in early data.

| | Inc. | VBF | Vh | $t\bar{t}h$ |
|----------------|------|-----|------|-------------|
| $\gamma\gamma$ | ✓ | ✓ | ✓ | ✓ |
| WW^* | ✓ | ✓ | ✓ | ✓ |
| ZZ^* | ✓ | ✓ | — | — |
| $\tau\tau$ | — | ✓ | — | — |
| $b\bar{b}$ | — | ✓ | ✓ | — |

One of the most natural questions to ask at this stage is to what accuracy the Higgs couplings may be extracted with a low luminosity data set. There have been several theory-level studies to this end in the past decade [4, 16–20]. Such theory studies must be treated with caution, since a detailed treatment of the actual systematic errors present in measurements of cross section times branching ratios, particularly in (ratios of) exclusive channels, is necessarily an experiment-level question. Nonetheless, they provide some rough guide of the approximate accuracy with which couplings and ratios might be measured at a given integrated luminosity. Of these, [4] is the most germane to the situation at hand, investigating the accuracy with which couplings and ratios of exclusive processes might be measured for a 125 GeV Higgs using 7.5 - 17.5 fb^{-1} of integrated luminosity at 7-8 TeV and 30 fb^{-1} of integrated luminosity at 14 TeV. The one sigma error bars for any given channel at 7-8 TeV with 17.5 fb^{-1} are larger than $\pm 20\%$ of the Standard Model value, with the hWW coupling measurable to within $\sim \pm 25\%$; the uncertainties for htt (hence also hgg), hbb , and $h\tau\tau$ couplings are $\mathcal{O}(1)$ fractions of the SM value. The prospects for exclusive ratios are similar, with the most promising ratio being that of g_{hZZ}/g_{hWW} . The $g_{h\tau\tau}/g_{hWW}$ should also be promising [20], measurable via the ratio of VBF exclusive production for the $h \rightarrow WW \rightarrow 2\ell 2\nu$ and $h \rightarrow \tau\tau$ final states. These projections provide a useful guide to the channels that may most strongly constrain deviations from SM couplings at low luminosity, but further detailed study is beyond the scope of the current work.

3 Extended Higgs sectors

In principle there are many possible extensions and deformations of the minimal Higgs sector. Here we restrict our focus to perhaps the simplest class of extensions: theories with two Higgs fields transforming as doublets under $SU(2)_L$ with unit $U(1)_Y$ charge. Such 2HDMs provide a general effective theory framework for extensions of the electroweak symmetry breaking sector, supersymmetric or otherwise. Of the eight real scalars present in a 2HDM, three are eaten by electroweak symmetry breaking, leav-

ing five physical scalars: with CP conservation, the CP even neutral Higgses h and H ; the CP odd pseudoscalar A ; and the charged Higgses H^\pm .

Given more than one Higgs doublet, a sufficient condition for the absence of tree-level FCNCs is guaranteed by the Glashow-Weinberg condition [21] that all fermions of a given gauge representation receive their mass through renormalizable couplings to precisely one Higgs doublet. In the case of two Higgs doublets (denoted Φ_1 and Φ_2), the Glashow-Weinberg condition is satisfied by precisely four discrete types of 2HDM distinguished by the possible assignments of fermion couplings. By convention Φ_2 is fixed to be the Higgs doublet that couples to $Q\bar{u}$. This leaves four possible choices of couplings to $Q\bar{d}$ and $L\bar{e}$. Of these four models, Type I with all fermions coupled to one doublet contains the fermi-phobic Higgs as a limit (in which the SM-like Higgs is isolated in the other doublet). Type II is MSSM-like, in that this is the only choice of charge assignments consistent with a holomorphic superpotential. What we choose to call Type III is also known as lepton-specific, since it assigns a Higgs doublet solely to leptons.² What we choose to call Type IV is also known as flipped, for the obvious reason that the leptons have a flipped coupling relative to Type II. These possible couplings are illustrated in Table 2; for a comprehensive review, see [22].

Table 2. Higgs boson couplings to $SU(2)_L$ singlet fermions in the four discrete types of 2HDM models that satisfy the Glashow-Weinberg condition.

| | 2HDM I | 2HDM II | 2HDM III | 2HDM IV |
|-----|----------|----------|----------|----------|
| u | Φ_2 | Φ_2 | Φ_2 | Φ_2 |
| d | Φ_2 | Φ_1 | Φ_2 | Φ_1 |
| e | Φ_2 | Φ_1 | Φ_1 | Φ_2 |

If we restrict ourselves to extended EWSB sectors with two Higgs doublets that satisfy the Glashow-Weinberg condition with no tree-level FCNCs, and CP conservation, then the renormalizable tree-level couplings of all five scalar degrees of freedom to Standard Model fermions and massive gauge bosons are fixed in terms of two parameters: the mixing angle α of the two CP even neutral mass eigenstates h, H ; and the angle β , which parameterizes the relative contribution of each doublet to EWSB via $\tan \beta \equiv \langle \Phi_2 \rangle / \langle \Phi_1 \rangle$. In particular, this involves no additional assumptions about the form of the full non-renormalizable scalar potential (beyond CP conservation). This is to be contrasted with (CP and flavor conserving) multi-Higgs theories for which the tree-level couplings to up- and down-type quarks, leptons, and massive gauge bosons are in general all independent. The general tree-level couplings of CP-conserving 2HDMs (with the Glashow-Weinberg condition) are therefore restricted to particular two-dimensional sub-spaces of the general four-dimensional space of Higgs couplings to the Standard Model fermions and massive gauge boson. This is also to be contrasted with the single Higgs theory with general non-renormalizable couplings in which the coupling to every Standard Model state is independent (with deviations from renormalizable couplings parameterized by non-renormalizable operators).

The two-parameter scalings of the neutral Higgs boson couplings to SM fermions and massive gauge bosons, relative to the SM values, for the four types of 2HDMs are shown in Table 3. This implies that partial widths for tree-level decays of the Higgs scalars to Standard Model final states

²To avoid confusion, we emphasize that this is distinct from the general 2HDM with flavor-violating couplings, often referred to in the literature as Type III. There also appears to be no universal convention relating the III and IV labels to lepton-specific and flipped 2HDM.

also depend only on α, β relative to SM Higgs partial widths. These relations are modified at the quantum level, but in the framework here such corrections are perturbatively small.³ Similarly, note that the loop-induced decay $h \rightarrow \gamma\gamma$ exhibits a very mild dependence on additional parameters, since the charged Higgs H^\pm may run in the loop along with Standard Model fields. However, unless the charged Higgses are particularly light, this effect is negligible compared to contributions from W and top loops, being suppressed relative to W and top loops by a factor of $\mathcal{O}(m_W^2/m_{H^\pm}^2)$. As such, in what follows we will neglect corrections from H^\pm to the $h \rightarrow \gamma\gamma$ rate.

Of course, the actual branching ratios of Higgs scalars to SM final states depend on the sum of their partial widths, which may include appreciable decays to other Higgs scalars that are sensitive to the details of the scalar potential. Nonetheless, if h is the lightest Higgs, then it has the same decay channels as the SM Higgs, with no additional decay modes. It also has the same production channels as the SM Higgs, though there may be additional contributions to production modes via heavy scalars; the size of these contributions depends on the masses and branching ratios of the heavy scalars. If these additional contributions are negligible, the observable production cross sections and branching ratios in standard Higgs channels of the scalar h are completely determined relative to the SM Higgs by the parameters α and β . In contrast, the branching ratios of the heavier scalar states depend on the mass orderings; we will reserve a discussion of these decays for Section 6.

Table 3. Tree-level couplings of the neutral Higgs bosons to up- and down-type quarks, leptons, and massive gauge bosons in the four types of 2HDM models relative to the SM Higgs boson couplings as a function of α and β .

| | 2HDM I | 2HDM II | 2HDM III | 2HDM IV |
|-------|----------------------------|-----------------------------|-----------------------------|-----------------------------|
| hVV | $\sin(\beta - \alpha)$ | $\sin(\beta - \alpha)$ | $\sin(\beta - \alpha)$ | $\sin(\beta - \alpha)$ |
| hQu | $\cos \alpha / \sin \beta$ | $\cos \alpha / \sin \beta$ | $\cos \alpha / \sin \beta$ | $\cos \alpha / \sin \beta$ |
| hQd | $\cos \alpha / \sin \beta$ | $-\sin \alpha / \cos \beta$ | $\cos \alpha / \sin \beta$ | $-\sin \alpha / \cos \beta$ |
| hLe | $\cos \alpha / \sin \beta$ | $-\sin \alpha / \cos \beta$ | $-\sin \alpha / \cos \beta$ | $\cos \alpha / \sin \beta$ |
| HVV | $\cos(\beta - \alpha)$ | $\cos(\beta - \alpha)$ | $\cos(\beta - \alpha)$ | $\cos(\beta - \alpha)$ |
| HQu | $\sin \alpha / \sin \beta$ | $\sin \alpha / \sin \beta$ | $\sin \alpha / \sin \beta$ | $\sin \alpha / \sin \beta$ |
| HQd | $\sin \alpha / \sin \beta$ | $\cos \alpha / \cos \beta$ | $\sin \alpha / \sin \beta$ | $\cos \alpha / \cos \beta$ |
| HLe | $\sin \alpha / \sin \beta$ | $\cos \alpha / \cos \beta$ | $\cos \alpha / \cos \beta$ | $\sin \alpha / \sin \beta$ |
| AVV | 0 | 0 | 0 | 0 |
| AQu | $\cot \beta$ | $\cot \beta$ | $\cot \beta$ | $\cot \beta$ |
| AQd | $-\cot \beta$ | $\tan \beta$ | $-\cot \beta$ | $\tan \beta$ |
| ALe | $-\cot \beta$ | $\tan \beta$ | $\tan \beta$ | $-\cot \beta$ |

Assuming the SM-like Higgs, h , is the lightest scalar, we may efficiently estimate the NLO production cross section and branching ratios for the light CP even neutral Higgs h in a 2HDM from known NLO rates for a Standard Model Higgs of the same mass by applying the LO coupling ratios as a function of α, β . For example, we may estimate NLO branching ratios via

$$\Gamma_{\text{NLO}}(X \rightarrow Y) \simeq \Gamma_{\text{NLO}}^{\text{SM}}(X \rightarrow Y) \frac{\Gamma_{\text{LO}}(X \rightarrow Y)}{\Gamma_{\text{LO}}^{\text{SM}}(X \rightarrow Y)}$$

³For recent studies of cases (such as certain limits of the MSSM) in which additional degrees of freedom beyond the 2HDM may significantly alter partial widths at one loop, see e.g. [23].

where the LO ratio $\Gamma_{\text{LO}}(X \rightarrow Y)/\Gamma_{\text{LO}}^{\text{SM}}(X \rightarrow Y)$ may be obtained by applying the parametric scalings in Table 3 to the relevant Standard Model processes. This procedure is straightforward for tree-level couplings, and may be extended to the leading-order loop-level couplings assuming only SM particles run in the loops [24]. Likewise, we may estimate the NLO production cross section for a given process via

$$\sigma_{\text{NLO}}(X \rightarrow Y) \simeq \sigma_{\text{NLO}}^{\text{SM}}(X \rightarrow Y) \frac{\Gamma_{\text{LO}}(X \rightarrow Y)}{\Gamma_{\text{LO}}^{\text{SM}}(X \rightarrow Y)}.$$

We obtain the cross sections for each SM Higgs boson production channel and branching ratios for a Higgs mass of 125 GeV from the LHC Higgs Cross Section Group [25]. In what follows, the cross sections for various channels are important largely for determining their relative weight in inclusive processes. For simplicity we focus on cross sections at 7 TeV, and note that the relative contributions of various channels do not change significantly between 7 and 8 TeV.

There are two key quantities that control much of the parametric behavior in various Higgs channels: the coupling of the Higgs to W and Z bosons, and the partial width $\Gamma(h \rightarrow b\bar{b})$. The VBF and Vh exclusive production $\sigma \cdot \text{Br}$ scale as $g_{hVV}^2 \propto \sin^2(\beta - \alpha)$, as does the partial width $\Gamma(h \rightarrow VV^*)$. As $\sin(\beta - \alpha) \rightarrow 1$, the vector boson production and decay modes of h approach those of the Standard Model Higgs, while the heavy neutral scalar H decouples. Thus $\sin^2(\beta - \alpha)$ – which is a universal scaling of the hVV^* partial width among the various 2HDM types – underlies much of the parametric behavior of key production and decay modes. We correspondingly designate $\sin(\beta - \alpha) \rightarrow 1$ as a decoupling limit, though in this case the decoupling limit does not imply anything about the masses of the scalars, only the couplings. A second useful quantity is the partial width $\Gamma(h \rightarrow b\bar{b})$, insofar as it is typically the dominant decay mode and controls the total width of the Higgs (assuming no significant decay products beyond the standard channels). Since the $\sigma \cdot \text{Br}$ for many standard Higgs channels is inversely proportional to the total width, the parametric behavior of the dominant $\Gamma(h \rightarrow b\bar{b})$ partial width typically governs the branching ratio for rare decays. These two quantities are shown in Figs. 1 and 2.

The parametric behavior of these quantities as a function of α and β often suffices to understand the scaling of various exclusive channels. In particular, this implies that the signals of Type 1 and Type 3 2HDM are similar to each other in most standard channels (particularly for di-photon and diboson final states, for both inclusive and exclusive production); the same is likewise true for Type 2 and Type 4 2HDM. These similarities arise because in each case the quark couplings are identical for the pairs of 2HDM, so in particular the scaling of the $h \rightarrow b\bar{b}$ partial widths (as well as the $h t\bar{t}$ couplings that governs the gluon fusion production rate) are identical. The only substantial distinction arises in standard channels with ditau final states, since the lepton couplings differ.

4 SM-like Higgs inclusive production

Inclusive production channels are likely to provide the first decisive evidence for the Higgs, in large part due to the size of the gg fusion production cross section. However, not all final states of the Higgs may be efficiently probed through inclusive production; high-background channels such as $h \rightarrow \tau\tau$ and $h \rightarrow b\bar{b}$ require additional discriminants such as forward jets or associated leptons in order to efficiently distinguish signal from background. Of the possible inclusive processes, the $h \rightarrow \gamma\gamma$ and various $h \rightarrow VV^*$ channels are the most promising, particularly $h \rightarrow WW^* \rightarrow 2\ell 2\nu$ and $h \rightarrow ZZ^* \rightarrow 4\ell$. These latter states all have identical parametric scaling in the 2HDM under consideration, so we may treat them collectively.

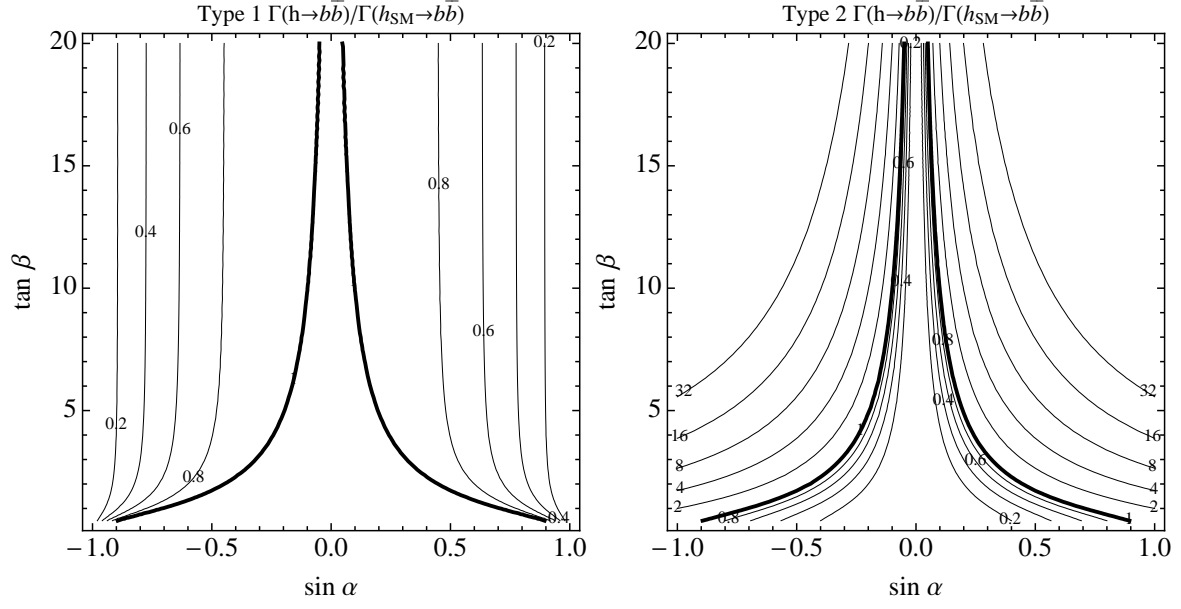


Figure 1. Contours of $\Gamma(h \rightarrow b\bar{b})/\Gamma(h_{SM} \rightarrow b\bar{b})$ for the SM-like Higgs boson as a function of $\sin \alpha$ and $\tan \beta$ in Type 1 2HDM (left) and Type 2 2HDM (right). The Type 3 model is parametrically similar to Type 1, while Type 4 is similar to Type 2. Thick black lines denote the SM value.

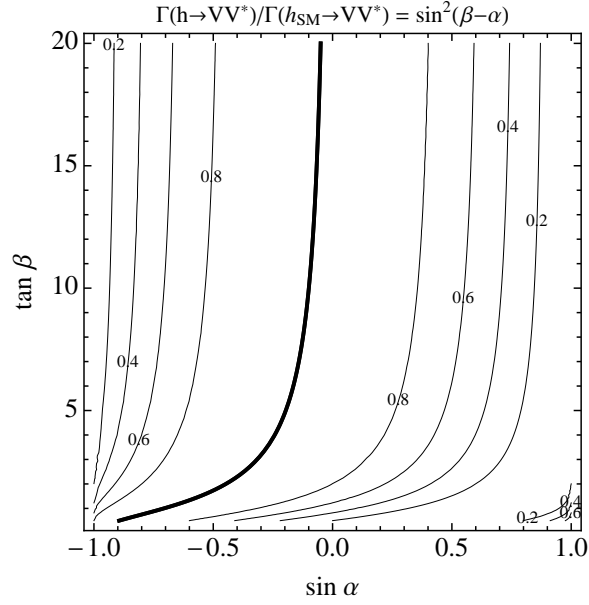


Figure 2. Contours of $\Gamma(h \rightarrow VV^{(*)})/\Gamma(h_{SM} \rightarrow VV^{(*)}) = \sin^2(\beta - \alpha)$ for the SM-like Higgs boson as a function of $\sin \alpha$ and $\tan \beta$ in any of the 2HDMs. Thick black lines denote the SM value corresponding to the $\sin^2(\beta - \alpha) = 1$ decoupling limit.

We approximate the inclusive production $\sigma \cdot \text{Br}$ by summing over the production cross sections

of various channels. This procedure does not account for possible differences in the experimental acceptance between various production channels. However, the corrections in this case due to unknown acceptance are at the very most $\mathcal{O}(\sigma_{qq'\rightarrow h}^{SM}/\sigma_{gg\rightarrow h}^{SM}) \sim 8\%$ and therefore do not qualitatively affect the conclusions.

4.1 Inclusive di-photon

The inclusive di-photon rate, on its own, is not necessarily a powerful discriminant of new physics. Nonetheless, as we will see below, it may prove useful in conjunction with precise measurements of certain exclusive channels.

We show contours of the inclusive $\sigma \cdot \text{Br}$ for $h \rightarrow \gamma\gamma$ in Type 1 and Type 2 2HDM relative to the Standard Model $\sigma \cdot \text{Br}$ in Fig. 3; the contours for Type 3 and Type 4 2HDM are respectively similar. In Type 1 and Type 3 2HDM, the contours of the inclusive di-photon $\sigma \cdot \text{Br}$ largely track the $g_{hVV} = \sin(\beta - \alpha)$ coupling, rather than the total width. Although the branching ratio $\text{Br}(h \rightarrow \gamma\gamma)$ increases in inverse proportionality to the total width, the $gg \rightarrow h$ production rate is directly proportional (in its functional dependence on the angles α, β) to the dominant $h \rightarrow b\bar{b}$ partial width, since the ggh coupling is proportional to the $ht\bar{t}$ coupling and both $g_{ht\bar{t}}, g_{hb\bar{b}} \propto \cos\alpha/\sin\beta$. As such, an increase in the di-photon branching ratio due to shrinking width is largely offset by a decrease in the production rate. Thus the dominant effect on the di-photon inclusive $\sigma \cdot \text{Br}$ comes from changes in the hVV coupling, which directly affects the partial width $\Gamma(h \rightarrow \gamma\gamma)$ since the coupling of the Higgs to photons is dominated by a W boson loop. Since the hVV coupling saturates at the Standard Model value, this suggests that the inclusive di-photon $\sigma \cdot \text{Br}$ in Type 1 and Type 3 models is typically bounded from above by the Standard Model rate. In contrast, in Type 2 and Type 4 2HDM, the contours of the inclusive di-photon $\sigma \cdot \text{Br}$ largely track the inverse total width. In these theories the $gg \rightarrow h$ production rate and total width are not strongly correlated, so that $\text{Br}(h \rightarrow \gamma\gamma)$ may increase as the total width drops, while the production rate $\sigma(gg \rightarrow h)$ remains fixed. Since the total width may grow arbitrarily small as $\Gamma(h \rightarrow b\bar{b})$ decreases, the inclusive di-photon $\sigma \cdot \text{Br}$ in Type 2 and Type 4 2HDM may be many times the Standard Model rate.

4.2 Inclusive VV^*

The parametric scaling of the inclusive $h \rightarrow VV^*$ $\sigma \cdot \text{Br}$ is quite similar to that of the inclusive di-photon rate, as shown in Fig. 4. In the case of Type 1 and Type 3 models, the inclusive $\sigma \cdot \text{Br}$ again decouples from the total width and largely tracks the partial width $\Gamma(h \rightarrow VV^*)$. Whereas the partial width in case of the inclusive di-photon $\sigma \cdot \text{Br}$ is a function of both hVV and $ht\bar{t}$ tree-level couplings, here it is simply a function of the hVV coupling, and so the dependence is somewhat sharper as a function of α and β . In Type 2 and Type 4 2HDM, as before, the inclusive $\sigma \cdot \text{Br}$ tracks the inverse width.

4.3 Inclusive ratios

In addition to the inclusive $\sigma \cdot \text{Br}$ themselves, we may consider measurements of the inclusive $\gamma\gamma/VV^*$ ratio, shown in Fig. 5. Dependence on the ggh coupling largely drops out of this ratio, as do many systematics. Given the considerable statistics available in the inclusive channels, this is likely to be the first ratio observed with any meaningful accuracy at the LHC. However, in a 2HDM this inclusive ratio is not particularly sensitive to deviations from SM couplings, due to the fact that both the $h\gamma\gamma$ and hVV^* partial widths scale in large part with the hVV coupling. Although the $h\gamma\gamma$ coupling obtains contributions from both W and top loops, the W contribution dominates; for an SM Higgs at

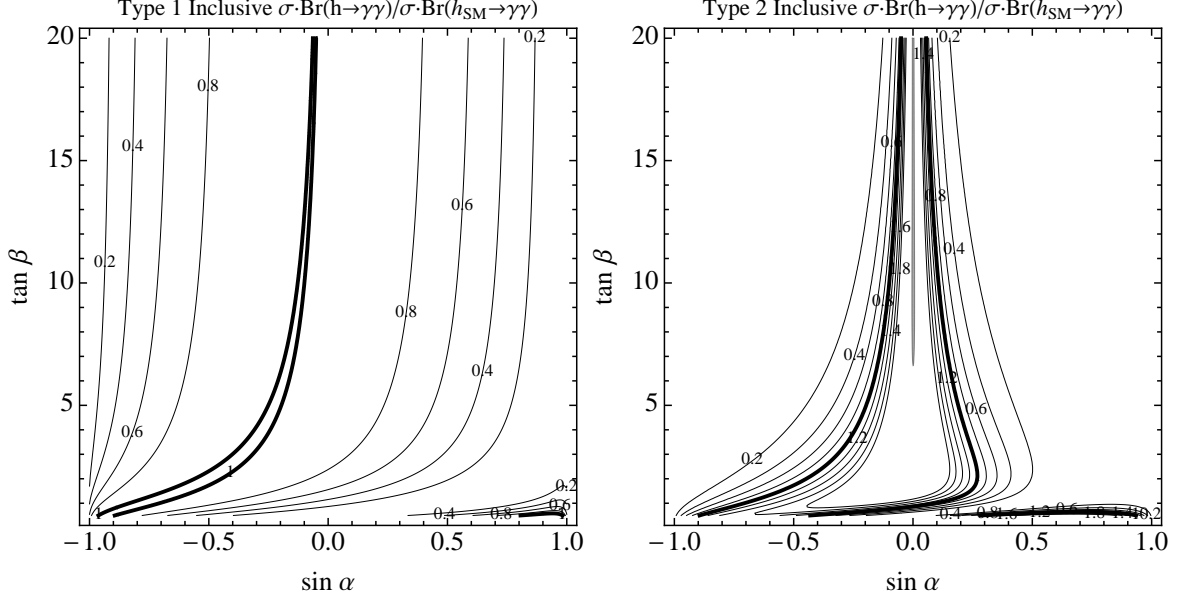


Figure 3. Contours of the inclusive $\sigma \cdot \text{Br}(h \rightarrow \gamma\gamma) / \sigma \cdot \text{Br}(h_{SM} \rightarrow \gamma\gamma)$ for the SM-like Higgs boson with $m_h = 125$ GeV as a function of $\sin \alpha$ and $\tan \beta$ in Type 1 2HDM (left) and Type 2 2HDM (right). The Type 3 model is parametrically similar to Type 1, while Type 4 is similar to Type 2. Thick black lines denote the SM value. The shaded gray region denotes a recent CMS inclusive $\sigma \cdot \text{Br}(h \rightarrow \gamma\gamma)$ exclusion for $m_h = 125$ GeV [9].

125 GeV the contribution from the top loop only amounts to $\sim 28\%$ of the total $h\gamma\gamma$ loop amplitude. As such, the variation in this inclusive ratio as a function of α, β is quite mild.

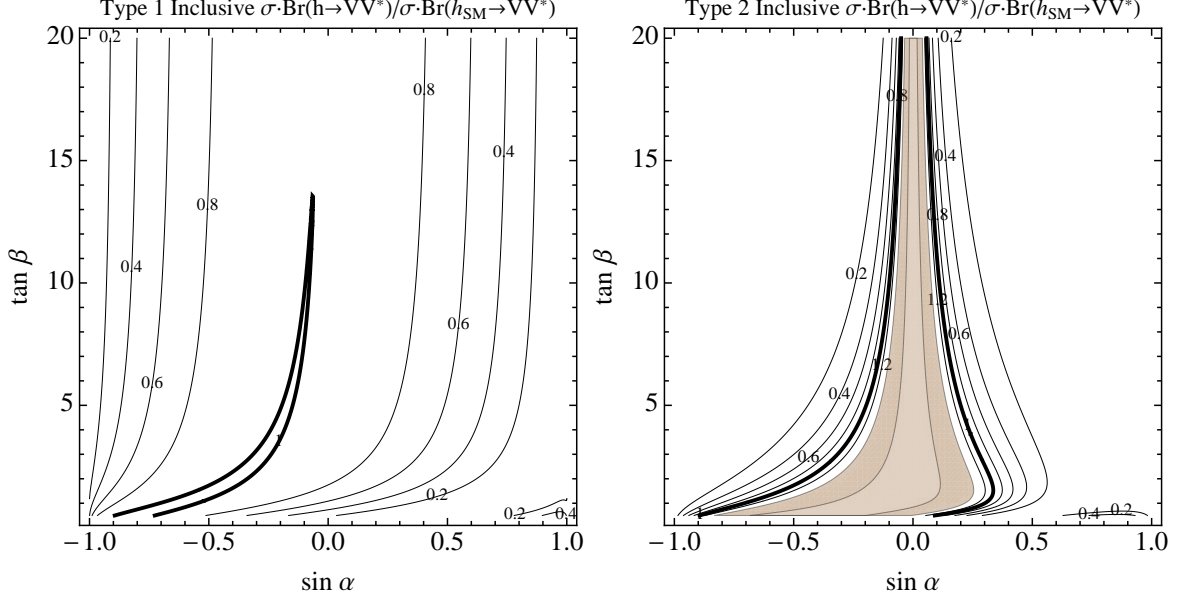


Figure 4. Contours of the inclusive $\sigma \cdot \text{Br}(h \rightarrow VV^*) / \sigma \cdot \text{Br}(h_{SM} \rightarrow VV^*)$ for the SM-like Higgs boson with $m_h = 125$ GeV as a function of $\sin \alpha$ and $\tan \beta$ in Type 1 2HDM (left) and Type 2 2HDM (right). The Type 3 model is parametrically similar to Type 1, while Type 4 is similar to Type 2. Thick black lines denote the SM value. The light and dark brown regions denote recent CMS inclusive $\sigma \cdot \text{Br}(h \rightarrow ZZ^* \rightarrow 4\ell)$ and $\sigma \cdot \text{Br}(h \rightarrow WW^* \rightarrow 2\ell 2\nu)$ exclusions respectively for $m_h = 125$ GeV [11, 13].

5 SM-like Higgs exclusive production

Although the cross section for exclusive channels beyond gluon fusion is more than an order of magnitude smaller than the inclusive cross section, the relatively lower backgrounds mean that many exclusive channels should eventually be observed. The most compelling exclusive channels are VBF and Vh associated production, with Standard Model cross sections at 7 TeV ranging from several hundred femtobarns in the case of Zh to more than one picobarn in the case of VBF. And while the cross section for $t\bar{t}h$ associated production is considerably smaller, it may also be observable in certain channels.

Exclusive channels are compelling not only because of the relatively low backgrounds and isolated production couplings, but also because they admit searches for Higgs final states that are inaccessible in inclusive measurements. In this respect, vector boson fusion with $h \rightarrow \tau\tau$ is particularly useful, both for differentiating 2HDM from the Standard Model Higgs and for distinguishing various types of 2HDM from each other. Note that the parametric behavior of several exclusive $\sigma \cdot \text{Br}$ are identical in 2HDM extensions of the Higgs sector; both vector boson fusion and Vh associated production arise from the same tree-level hVV coupling, so these exclusive production modes scale identically and may be treated collectively. Likewise, for exclusive channels there is less ambiguity relating to adding channels with unknown acceptances.

5.1 Exclusive VBF/ Wh / Zh di-photon

The exclusive VBF di-photon $\sigma \cdot \text{Br}$ is a primary discriminant between 2HDM and the Standard Model Higgs. The inclusive and VBF di-photon signals are observable at low integrated luminosity, and a

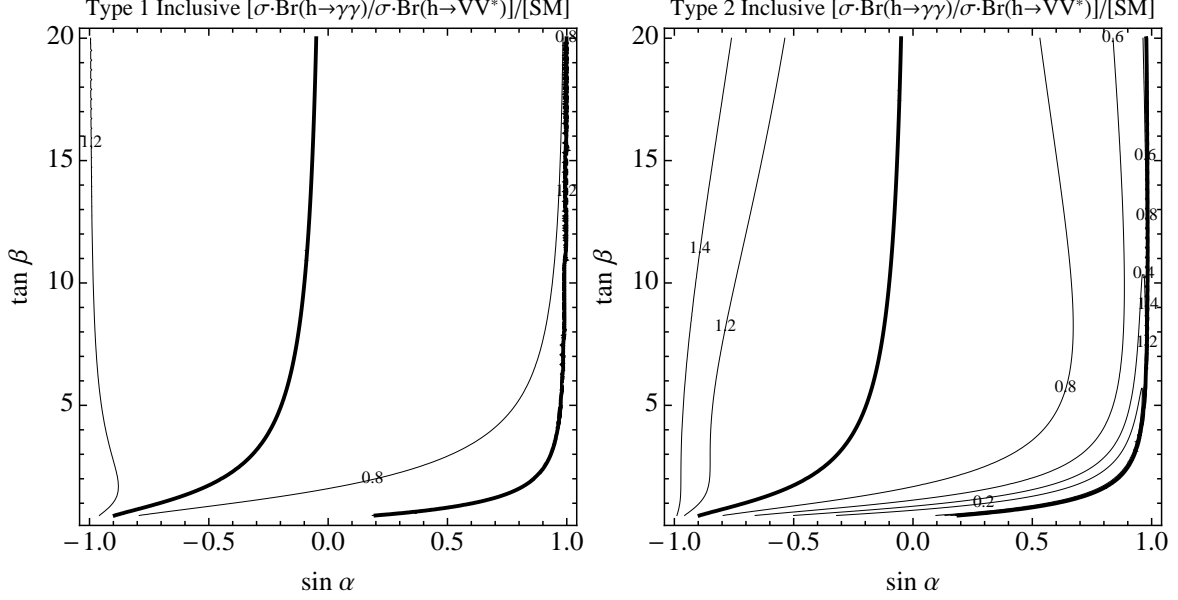


Figure 5. Contours of the inclusive ratio $[\sigma \cdot \text{Br}(h \rightarrow \gamma\gamma)/\sigma \cdot \text{Br}(h \rightarrow VV^*)]/[\sigma \cdot \text{Br}(h_{SM} \rightarrow \gamma\gamma)/\sigma \cdot \text{Br}(h_{SM} \rightarrow VV^*)]$ for the SM-like Higgs boson with $m_h = 125$ GeV as a function of $\sin \alpha$ and $\tan \beta$ in Type 1 2HDM (left) and Type 2 2HDM (right). The Type 3 model is parametrically similar to Type 1, while Type 4 is similar to Type 2. Thick black lines denote the SM value.

comparison of inclusive and exclusive $\sigma \cdot \text{Br}$ may provide one of the earliest indications of discrepant Higgs couplings.

Ratios of the exclusive VBF di-photon $\sigma \cdot \text{Br}$ relative to the Standard Model are shown in Fig. 6. In Type 1 and 3 2HDM, the exclusive di-photon $\sigma \cdot \text{Br}$ largely tracks the inclusive rate, except in the case of low $\tan \beta$ and large mixing, $-0.5 \gtrsim \sin \alpha \gtrsim -1$. In this region of parameter space, the VBF di-photon $\sigma \cdot \text{Br}$ may be significantly enhanced, while the inclusive $\sigma \cdot \text{Br}$ is consistent with the SM expectation. The reason for this enhancement is that here the total width of the Higgs drops well below the Standard Model value, raising the di-photon branching ratio. The ggh coupling drops at the same rate as the width, keeping the inclusive $\sigma \cdot \text{Br}$ more or less constant, but the hVV coupling remains large (since $\sin^2(\beta - \alpha) \sim 1$), so the VBF di-photon $\sigma \cdot \text{Br}$ is parametrically enhanced. Thus the inclusive $\sigma \cdot \text{Br}$ saturates at the SM value, while the VBF di-photon $\sigma \cdot \text{Br}$ may be enhanced over the SM $\sigma \cdot \text{Br}$ by as much as a factor of four. In contrast, in Type 2 and 4 2HDM the inclusive and VBF di-photon $\sigma \cdot \text{Br}$ are strongly correlated, and any enhancement or diminution in the VBF di-photon $\sigma \cdot \text{Br}$ points to equally enhanced inclusive rate. Unlike in the previous case, the decrease in width is parametrically distinct from the ggh effective coupling, so both the inclusive and VBF di-photon $\sigma \cdot \text{Br}$ are enhanced by a lower total width. Thus a large inclusive di-photon $\sigma \cdot \text{Br}$ typically points to a Type 2 or Type 4 2HDM, accompanied by a likely enhancement of the VBF di-photon rate. In contrast, a large VBF di-photon $\sigma \cdot \text{Br}$ and SM or smaller inclusive di-photon $\sigma \cdot \text{Br}$ would be strongly suggestive of a Type 1 or 3 2HDM. This is exemplified in Fig. 7, which shows the relative range of possible inclusive and VBF di-photon signals in 2HDM.

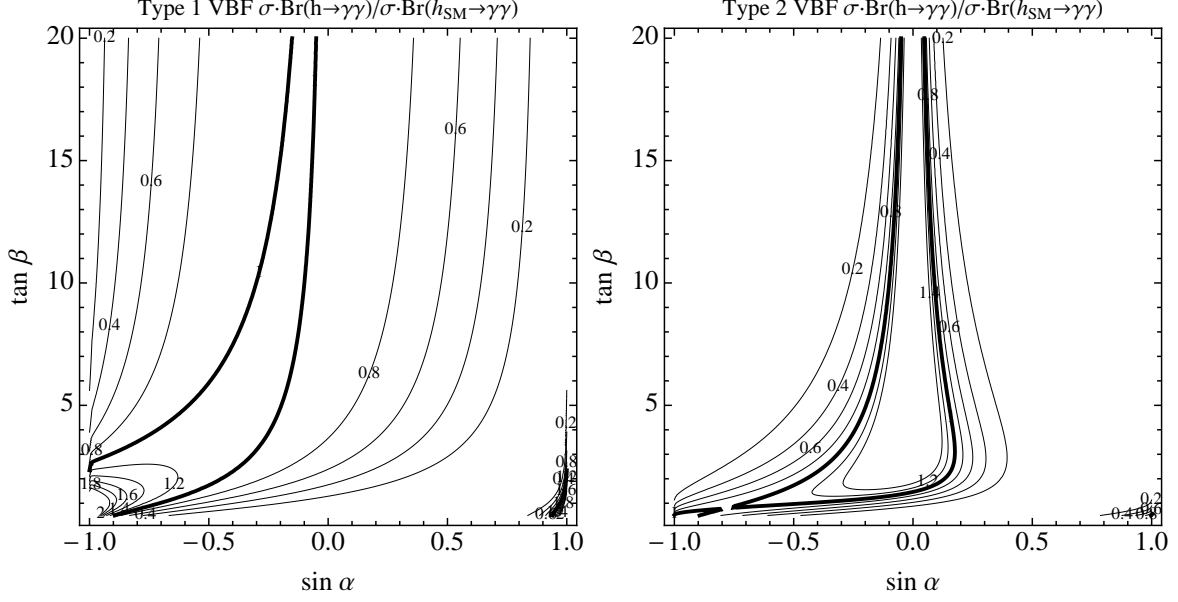


Figure 6. Contours of $\sigma\text{-Br}(V\text{BF or } Vh \rightarrow \gamma\gamma)/\sigma\text{-Br}(V\text{BF or } Vh_{SM} \rightarrow \gamma\gamma)$ for the SM-like Higgs boson as a function of $\sin \alpha$ and $\tan \beta$ in Type 1 2HDM (left) and Type 2 2HDM (right). The Type 3 model is parametrically similar to Type 1, while Type 4 is similar to Type 2. Thick black lines denote the SM value.

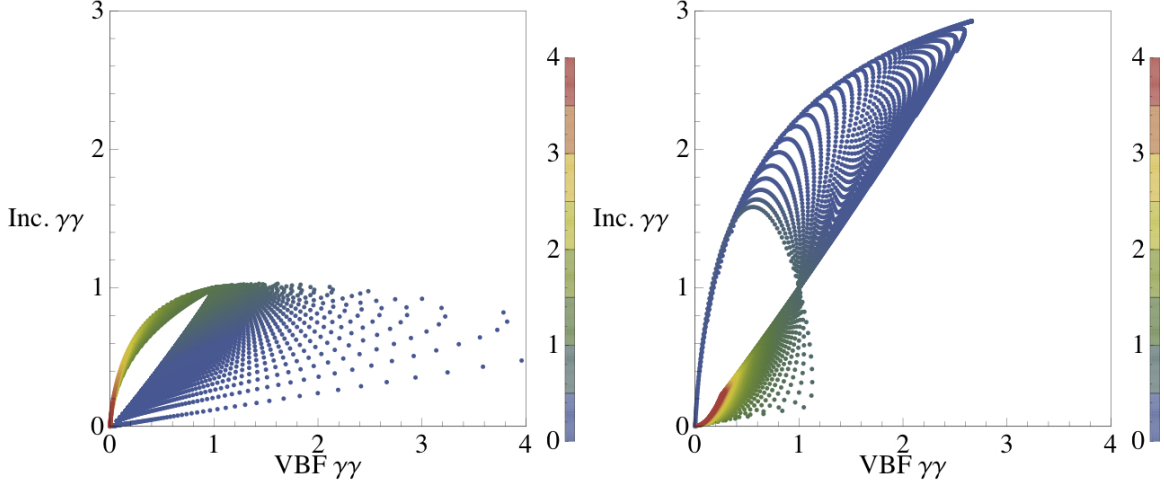


Figure 7. Scatter plot of the inclusive $\sigma\text{-Br}(h \rightarrow \gamma\gamma)/\sigma\text{-Br}(h_{SM} \rightarrow \gamma\gamma)$ as a function of $\sigma\text{-Br}(V\text{BF or } Vh \rightarrow \gamma\gamma)/\sigma\text{-Br}(V\text{BF or } Vh_{SM} \rightarrow \gamma\gamma)$ for the SM-like Higgs boson with $m_h = 125$ GeV as a function of $\sin \alpha$ and $\tan \beta$ in Type 1 2HDM (left) and Type 2 2HDM (right). The Type 3 model is parametrically similar to Type 1, while Type 4 is similar to Type 2. The points are colorized according to the SM-like Higgs total width relative to the Standard Model Higgs, $\Gamma(h \rightarrow \text{All})/\Gamma(h_{SM} \rightarrow \text{All})$, making clear that $\sigma\text{-Br}(V\text{BF or } Vh \rightarrow \gamma\gamma)$ is anti-correlated with the total width in both 2HDMs. The points are taken from a uniformly spaced grid in $-1 \leq \sin \alpha \leq 0$ and $0.5 \leq \tan \beta \leq 10$ with spacing $\Delta(\sin \alpha) = 0.01$ and $\Delta(\tan \beta) = 0.1$.

5.2 Exclusive VBF/ Wh/Zh VV^*

Much as in the case of inclusive processes, the exclusive channels with $h \rightarrow VV^*$ exhibit a parametric behavior similar to their $h \rightarrow \gamma\gamma$ counterparts, albeit with a slightly smaller SM-like region due to the sensitivity of the tree-level production couplings. In this sense, the exclusive channels with massive gauge boson final states provide a good cross-check of the di-photon $\sigma \cdot \text{Br}$. For example, an enhanced VBF di-photon $\sigma \cdot \text{Br}$ and SM-like inclusive $\sigma \cdot \text{Br}$ should be accompanied by correspondingly enhanced VBF and Vh diboson $\sigma \cdot \text{Br}$ with SM-like inclusive cross sections.

5.3 Exclusive VBF $\tau\tau$

The VBF $h \rightarrow \tau\tau$ $\sigma \cdot \text{Br}$ may provide one of the most sensitive discriminants for extended Higgs sectors, both relative to the Standard Model Higgs and among the various types of 2HDM. Ratios of the VBF $h \rightarrow \tau\tau$ $\sigma \cdot \text{Br}$ relative to the Standard Model expectation are shown in Fig. 8; let us briefly consider the different cases. In a Type 1 model, the $h \rightarrow \tau\tau$ exclusive production $\sigma \cdot \text{Br}$ in VBF is not expected to exceed the Standard Model rate, and in many cases will be significantly smaller. Moreover, the $h \rightarrow \tau\tau$ $\sigma \cdot \text{Br}$ will typically be SM-like if inclusive di-photon is SM-like. This occurs because the partial width $\Gamma(h \rightarrow \tau\tau)$ scales with the total width, so that the branching ratio is largely constant until the width grows small and the $\Gamma(h \rightarrow VV)$ partial widths take over. The production cross section lowers as the hVV coupling drops.

In a Type 2 model, the $h \rightarrow \tau\tau$ exclusive production $\sigma \cdot \text{Br}$ is not expected to exceed SM by more than $\sim 40\%$ for $\tan\beta < 20$, as apparent in Fig. 8. If the inclusive di-photon $\sigma \cdot \text{Br}$ is SM-like or larger, the $h \rightarrow \tau\tau$ exclusive $\sigma \cdot \text{Br}$ will be SM-like or smaller. This occurs because the $h\tau\tau$ coupling is parametrically identical to the $hb\bar{b}$ coupling, which dominates the total width; if the total width is suppressed, leading to enhanced inclusive di-photon signals, the $h \rightarrow \tau\tau$ branching ratio drops.

In a Type 3 model, the $h \rightarrow \tau\tau$ exclusive may be many times the SM value, independent of the inclusive di-photon rate. As before, the inclusive di-photon $\sigma \cdot \text{Br}$ saturates at the SM value due to the countervailing effects of the width and the ggh coupling. However, in contrast to the Type 1 model, in the Type 3 2HDM the $\Gamma(h \rightarrow \tau\tau)$ partial width grows as the total width drops, so that the branching ratio may be considerably enhanced.

Finally, in a Type 4 model, the $h \rightarrow \tau\tau$ $\sigma \cdot \text{Br}$ tracks the inclusive di-photon $\sigma \cdot \text{Br}$ closely. In Fig. 8 we see it may greatly exceed the SM value, but an enhanced $\sigma \cdot \text{Br}$ is typically accompanied by an equally enhanced inclusive di-photon rate. Again, this arises because the $\Gamma(h \rightarrow \tau\tau)$ partial width grows as the total width drops, enhancing the branching ratio by the same effect that enhances the inclusive di-photon rate.

Now one may begin to see clearly the way in which patterns of exclusive $\sigma \cdot \text{Br}$ may begin to decisively differentiate between various types of 2HDM. As seen in Fig. 9, discrepancies in the inclusive and exclusive di-photon $\sigma \cdot \text{Br}$ provide a clear distinction between Type 1,3 and Type 2,4 models. In the former, the inclusive $\sigma \cdot \text{Br}$ is Standard Model or smaller while the exclusive di-photon $\sigma \cdot \text{Br}$ may be significantly enhanced; in the latter, the inclusive and exclusive $\sigma \cdot \text{Br}$ scale together. If these two classes of 2HDM are distinguished by the inclusive and exclusive di-photon $\sigma \cdot \text{Br}$, the particular type of 2HDM may be determined by the exclusive ditau rate. For a Type 1 2HDM the ditau $\sigma \cdot \text{Br}$ is SM or smaller, while in the Type 3 2HDM it is typically enhanced; the same is true of Type 2 and Type 4 models, respectively. Thus these three measurements – the inclusive di-photon, exclusive di-photon, and exclusive ditau $\sigma \cdot \text{Br}$ – may conceivably distinguish among 2HDM models in the event of discrepancies from the Standard Model expectations. Fortunately, they will be among the first processes to be observed.

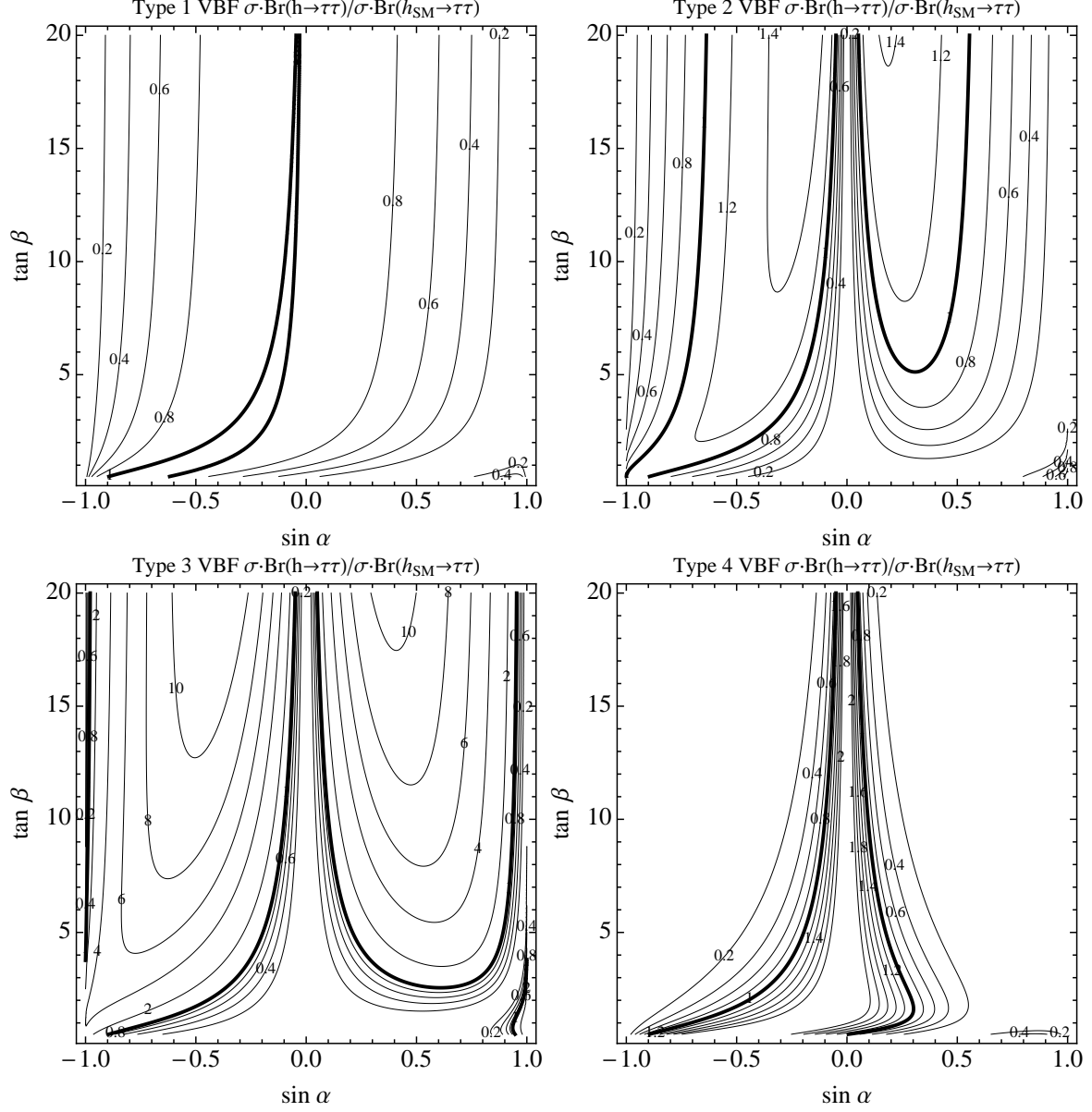


Figure 8. Contours of $\sigma \cdot \text{Br}(\text{VBF or } Vh \rightarrow \tau\tau) / \sigma \cdot \text{Br}(\text{VBF or } Vh_{SM} \rightarrow \tau\tau)$ for the SM-like Higgs boson as a function of $\sin \alpha$ and $\tan \beta$ in Type 1 2HDM (upper left), Type 2 2HDM (upper right), Type 3 2HDM (lower left), Type 4 2HDM (lower right). Thick black lines denote the SM value.

5.4 Exclusive VBF/ Wh $b\bar{b}$

It is further useful to consider exclusive channels with $h \rightarrow b\bar{b}$. The parametric scaling in the Type 1 and Type 3 2HDM is analogous to the Type 1 ditau rate, while that of the Type 2 and Type 4 2HDM is analogous to the Type 2 ditau rate. In this sense, the $h \rightarrow b\bar{b}$ and $h \rightarrow \tau\tau$ exclusive $\sigma \cdot \text{Br}$ provide a further discriminant between the 2HDM types, though the observation of the $h \rightarrow b\bar{b}$ final state is likely to lag the other exclusive channels somewhat.

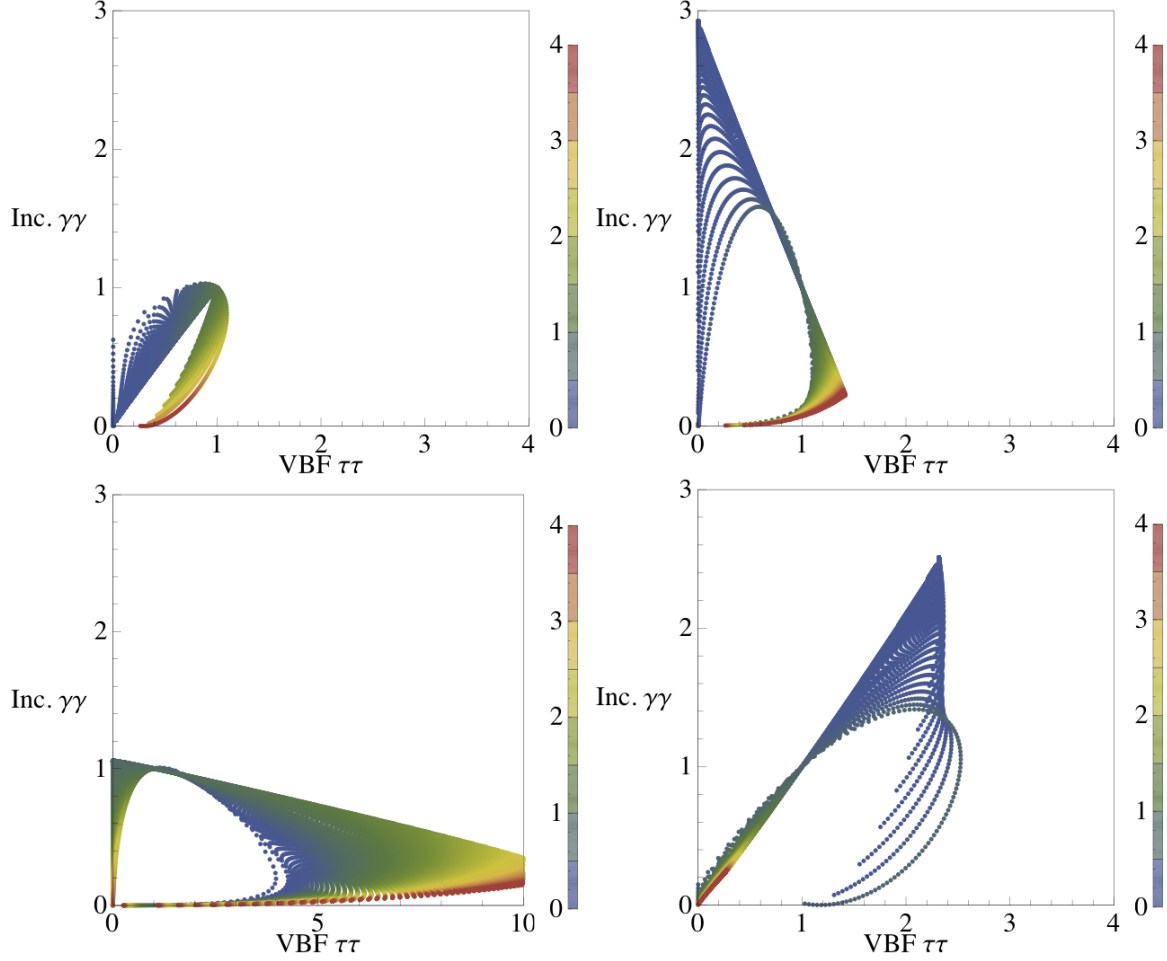


Figure 9. Scatter plot of the inclusive $\sigma \cdot \text{Br}(h \rightarrow \gamma\gamma)/\sigma \cdot \text{Br}(h_{SM} \rightarrow \gamma\gamma)$ as a function of $\sigma \cdot \text{Br}(\text{VBF or } Vh \rightarrow \tau\tau)/\sigma \cdot \text{Br}(\text{VBF or } Vh_{SM} \rightarrow \tau\tau)$ for the SM-like Higgs boson with $m_h = 125$ GeV as a function of $\sin \alpha$ and $\tan \beta$ in Type 1 2HDM (upper left), Type 2 2HDM (upper right), Type 3 2HDM (lower left), Type 4 2HDM (lower right). The points are colorized according to the SM-like Higgs total width relative to the Standard Model Higgs, $\Gamma(h \rightarrow \text{All})/\Gamma(h_{SM} \rightarrow \text{All})$. Note that the range for $\sigma \cdot \text{Br}(\text{VBF or } Vh \rightarrow \tau\tau)/\sigma \cdot \text{Br}(\text{VBF or } Vh_{SM} \rightarrow \tau\tau)$ differs for the Type 3 2HDM. The points are taken from a uniformly spaced grid in $-1 \leq \sin \alpha \leq 0$ and $0.5 \leq \tan \beta \leq 10$ with spacing $\Delta(\sin \alpha) = 0.01$ and $\Delta(\tan \beta) = 0.1$.

5.5 Exclusive $t\bar{t}h$ di-photon

Finally, let us consider the $t\bar{t}h$ di-photon channel, for which contours relative to the Standard Model are shown in Fig. 10. The parametric scaling for various 2HDM types is much like the inclusive di-photon scaling, since the production couplings have the same dependence on α, β as the $t\bar{t}$ contribution to the ggh effective coupling. In this sense, $t\bar{t}h$ provides a good cross-check of the inclusive di-photon rate, though of course the $t\bar{t}h$ di-photon signal will be relatively small.

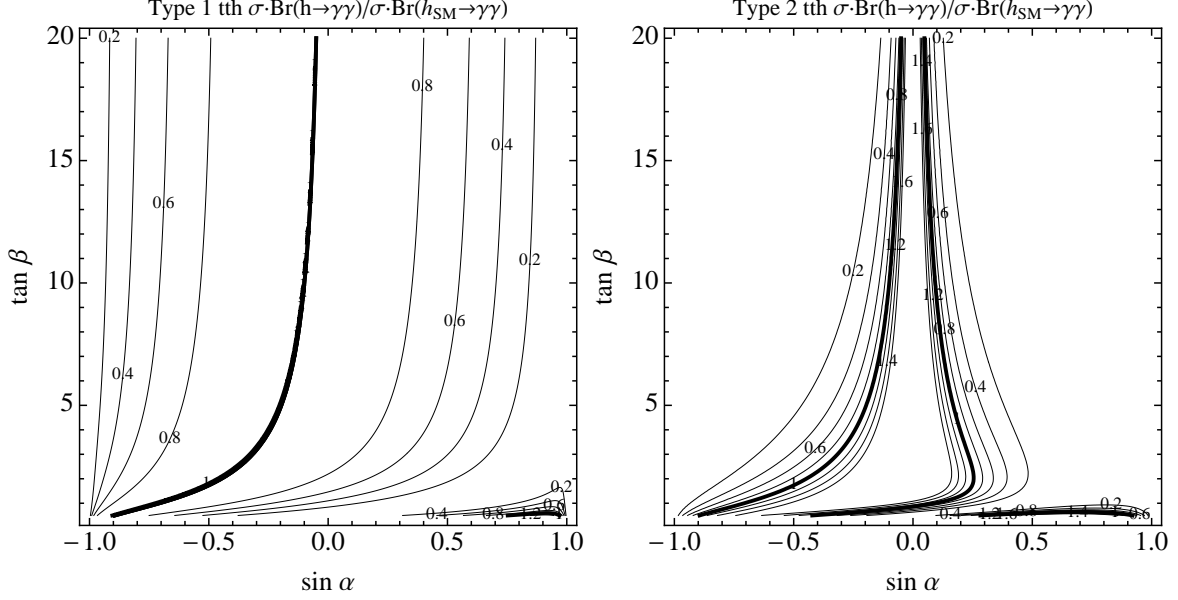


Figure 10. Contours of $\sigma \cdot \text{Br}(tth \rightarrow \gamma\gamma) / \sigma \cdot \text{Br}(tth_{\text{SM}} \rightarrow \gamma\gamma)$ for the SM-like Higgs boson as a function of $\sin \alpha$ and $\tan \beta$ in Type 1 2HDM (left) and Type 2 2HDM (right). Thick black lines denote the SM value.

5.6 Exclusive ratios

Although a side-by-side comparison of various inclusive and exclusive $\sigma \cdot \text{Br}$ provides considerable discrimination between various 2HDM types, each channel is accompanied by its own particular systematic errors. These errors reduce the significance of any departures from Standard Model expectations, making it unlikely that decisive observations of new physics can be made with low luminosity for all but the most extreme cases. Thus it is useful to examine certain exclusive ratios. Various systematics drop out of ratios of the same exclusive production channel with different final states, making such ratios sensitive to deviations in Higgs decays.

The parametric scaling of the VBF $\gamma\gamma/VV$ exclusive ratio is much like that of the inclusive $\gamma\gamma/VV$ ratio, and we need not reproduce the figure here. Far more interesting is the VBF $\tau\tau/\gamma\gamma$ exclusive ratio. Unsurprisingly, given the discriminating power of the $h \rightarrow \tau\tau$ final state, this exclusive ratio is fairly sensitive, varying rapidly from the Standard Model ratio in all types of 2HDM models as illustrated in Fig. 11. Finally, the VBF $\tau\tau/VV$ exclusive ratio has similar parametric behavior to the $\tau\tau/\gamma\gamma$ exclusive ratio. This exclusive ratio is particularly attractive, as theory studies of Higgs coupling measurements suggest this will be one of the earliest exclusive ratios to be probed at the LHC [20].

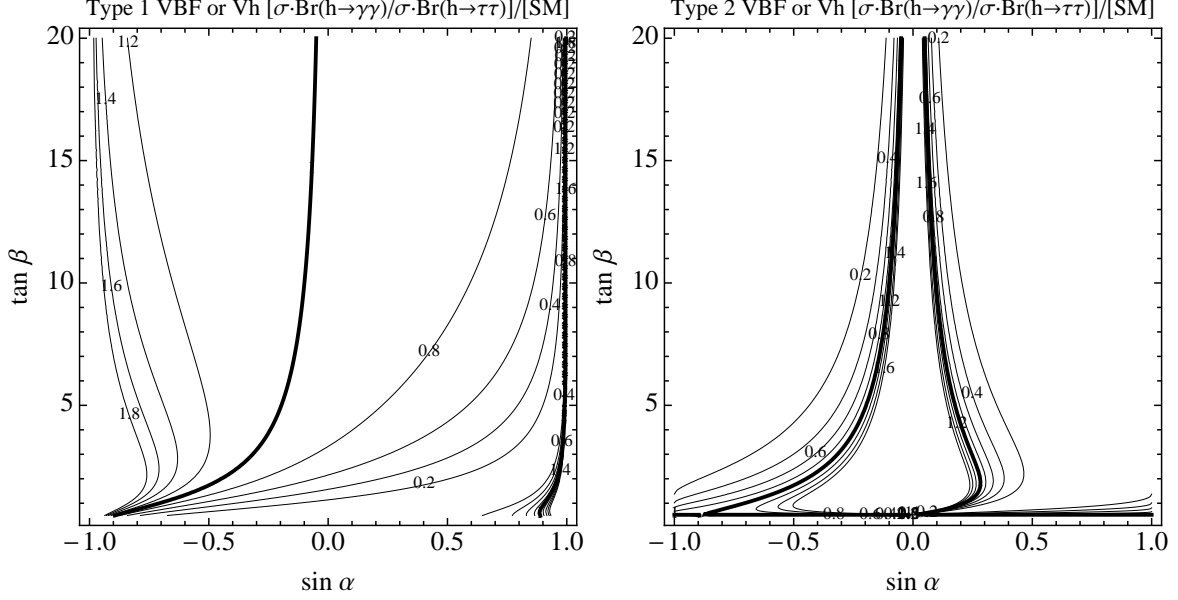


Figure 11. Contours of $[\sigma \cdot \text{Br}(\text{VBF or } Vh \rightarrow \gamma\gamma) / \sigma \cdot \text{Br}(\text{VBF or } Vh \rightarrow \tau\tau)] / [\sigma \cdot \text{Br}(\text{VBF or } Vh_{SM} \rightarrow \gamma\gamma) / \sigma \cdot \text{Br}(\text{VBF or } Vh_{SM} \rightarrow \tau\tau)]$ for the SM-like Higgs boson as a function of $\sin \alpha$ and $\tan \beta$ in Type 1 2HDM (left) and Type 2 2HDM (right). Thick black lines denote the SM value.

6 Heavy non-SM-like scalars

Thus far we have restricted our attention entirely to the SM-like CP even neutral scalar h , since its properties will initially merit the closest scrutiny. However, the other states present in 2HDMs may likewise appear in standard Higgs search channels, and their production rates can be constrained by existing Higgs searches. Of the various non-SM like Higgs states, the CP even neutral scalar H and the CP odd neutral scalar A are the most likely to appear in standard Higgs channels. The H is produced through both gluon-gluon fusion and all of the associated production channels, and could in principle be visible in the decay modes $H \rightarrow VV$, particularly $H \rightarrow WW \rightarrow 2\ell 2\nu$ and $H \rightarrow ZZ \rightarrow 4\ell, 2\ell 2\nu, 2\ell 2j, 2\ell 2\tau$, as well as $H \rightarrow \gamma\gamma$. With CP conservation, the pseudoscalar A has zero tree-level coupling to Standard Model gauge bosons, although it does possess the loop-level $A\gamma\gamma$ and Agg effective couplings. As such, the pseudoscalar is produced only through gluon-gluon fusion and $t\bar{t}A$ associated production. Likewise, it lacks the $A \rightarrow VV$ final states of high-mass standard Higgs searches, and so among the standard Higgs search channels it could in principle be visible in the $A \rightarrow \gamma\gamma$ decay mode. Note that the $A \rightarrow \tau\tau$ decay mode may also be significant, but because it does not occur in associated production, it's unlikely to appear in standard channels at low luminosity.

Of course, it is also possible for the non-SM like states to manifest themselves primarily in scalar cascade decays, ending in Standard Model final states plus the light SM-like Higgs h . These cascades may appear in standard Higgs channels as an enhancement of associated production processes. For example, the process $gg \rightarrow A \rightarrow Zh$ may have a sizable cross section, and appears as an enhancement of the Zh exclusive channel (albeit with boosted kinematics). In general, these scalar decays are highly model-dependent; their rates depend on unknown free parameters in the scalar potential that determine the Higgs self couplings, and on the masses of the various scalar states. Insofar as our focus lies on signatures appearing in standard Higgs channels, we will not give these scalar cascade signals

further consideration here.

Needless to say, the production cross sections and branching ratios for the heavy scalars depend sensitively on their masses and partial decay widths to any non-Standard Model states. However, in the limit where their decay widths are dominated by Standard Model final states, we can make quantitatively accurate statements about the cross section times branching ratios of these states relative to the Standard Model Higgs of the same mass. This is not an unreasonable approximation in many regions of parameter space, and more generally provides an upper limit on the size of signals measurable in standard Higgs channels. Once the masses of the heavy Higgses are above the top quark threshold, $2m_t$, their branching ratios to Standard Model final states vary slowly since the dominant partial width to $t\bar{t}$ varies slowly with the scalar mass.

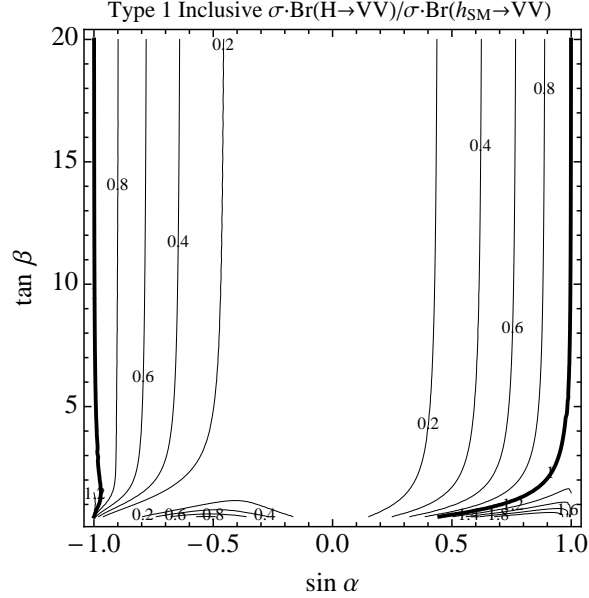


Figure 12. Contours of the inclusive $\sigma \cdot \text{Br}(H \rightarrow VV) / \sigma \cdot \text{Br}(h_{SM} \rightarrow VV)$ for the non-SM-like scalar Higgs boson assuming decays to Standard Model fermions and gauge bosons only as a function of $\sin \alpha$ and $\tan \beta$ in Type 1 2HDM with $m_H = m_{h_{SM}} = 400$ GeV. Thick black lines denote the SM value. Contours for other types of 2HDM are similar.

The inclusive diboson $\sigma \cdot \text{Br}$ for the heavy scalar H to VV is similar among the various types of 2HDM, as shown in Fig. 12 for $m_H = 400$ GeV, normalized to the $\sigma \cdot \text{Br}$ of a Standard Model Higgs of the same mass. This is due in large part to the fact that the width at high mass is dominated by top and vector boson final states, which have the same parametric scalings in all the types of 2HDM (with a mild exception at large $\tan \beta$ where $h \rightarrow b\bar{b}$ becomes important for the Type 2 and Type 4 2HDM). What is particularly apparent in Fig. 12 is the SM Higgs-like inclusive $\sigma \cdot \text{Br}$ (compared to a SM Higgs at that mass) in the limit $\sin \alpha \rightarrow \pm 1$. These are exceptionally interesting regions of parameter space, insofar as it is also in this limit that many of the standard channel $\sigma \cdot \text{Br}$ of h differ widely from the Standard Model value, particularly at small $\tan \beta$. Even away from these limits, the $\sigma \cdot \text{Br}$ for $H \rightarrow VV$ can be a sizeable fraction of the value for a SM Higgs boson of the same mass. So standard Higgs searches for VV final states for masses even well above the SM-like Higgs mass, can be useful probes of 2HDMs. The correlated complementary nature of $h \rightarrow VV^*$ and $H \rightarrow VV$ processes in a 2HDM can

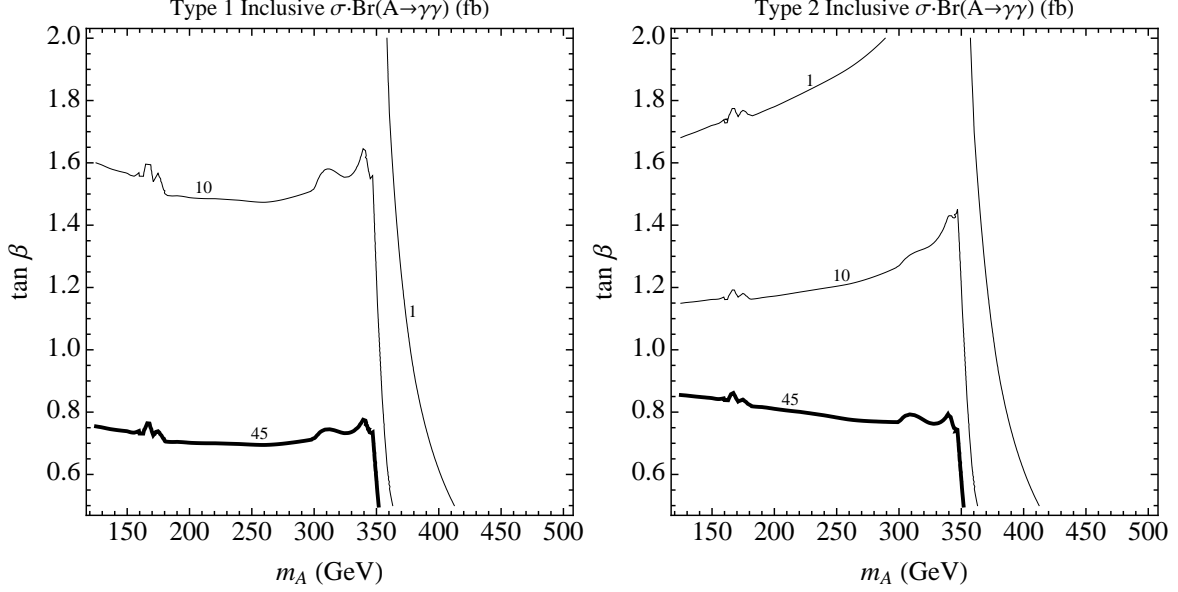


Figure 13. Contours of the inclusive $\sigma \cdot \text{Br}(A \rightarrow \gamma\gamma)$ in units of fb for 8 TeV pp collisions for the pseudo-scalar Higgs boson as a function of $\tan\beta$ and m_A in Type 1 2HDM (left) and Type 2 2HDM (right) assuming decays to Standard Model fermions and gauge bosons only. For reference the thick black lines are close to the SM value $\sigma \cdot \text{Br}(h_{SM} \rightarrow \gamma\gamma) \simeq 45$ fb for $m_h = 125$ GeV. Contours for Type 3 2HDM are similar to Type 1, and Type 4 2HDM to Type 2. The rapid drop in $\sigma \cdot \text{Br}(A \rightarrow \gamma\gamma)$ for $m_A \gtrsim 2m_t$ is due to the top quark threshold.

be seen by comparing Figs. 4 and 12. A sizeable deviation of $\sigma \cdot \text{Br}$ for $h \rightarrow VV^*$ from SM expectations implies a sizeable signal for $H \rightarrow VV$ (relative to a SM Higgs boson of the same mass). Conversely good agreement of $\sigma \cdot \text{Br}$ for $h \rightarrow VV^*$ with the SM expectation implies a reduced signal for $H \rightarrow VV$.

The production and decay modes of the pseudoscalar A depend only on $\tan\beta$ through its couplings to fermions, and are independent of the scalar mixing angle α . The inclusive di-photon $\sigma \cdot \text{Br}$ for A is shown in Fig. 13 as a function of $\tan\beta$ and the pseudoscalar mass. This $\sigma \cdot \text{Br}$ decreases rapidly with $\tan\beta$, since both the production and decay rates depend on the square of the $t\bar{t}A$ coupling. But at small $\tan\beta$ the di-photon signals of the pseudoscalar may be several times larger than a Standard Model Higgs of equivalent mass. Existing searches for 2HDM focus on τ -lepton final states of either the charged Higgs H^\pm coming from top quark decay or A and H produced in association with b -quarks. These searches are sensitive to large $\tan\beta$, and so the inclusive $A \rightarrow \gamma\gamma$ channel provides an interesting complementary probe of low $\tan\beta$.

The di-photon $\sigma \cdot \text{Br}$ for the heavy scalar H can be similar in magnitude to that of the pseudoscalar A , though in general it depends on both α and β . However, in the $\sin^2(\beta - \alpha) = 1$ decoupling limit it depends at most on $\tan\beta$ since H couples only to fermions in this limit. And the specific form of the dependence is rather simple because in any of the 2HDMs the magnitude and $\tan\beta$ dependence of the coupling of H to a given type of fermion is identical to that of the A . Consider first the ratio $\sigma \cdot \text{Br}(H \rightarrow \gamma\gamma) / \sigma \cdot \text{Br}(A \rightarrow \gamma\gamma)$ for H and A of the same mass in the Type 1 2HDM shown in Fig. 14. The ratio in the decoupling limit in this case is independent of $\tan\beta$ since the H and A couplings to all fermions are homogeneous in Type 1. Below the top threshold this ratio depends mainly on the overall coefficient of the fermion loop diagrams. Above the top threshold the relative di-photon branching ratio is larger for A than H since the $A \rightarrow t\bar{t}$ decay is P-wave suppressed, while $H \rightarrow t\bar{t}$ is S-wave.

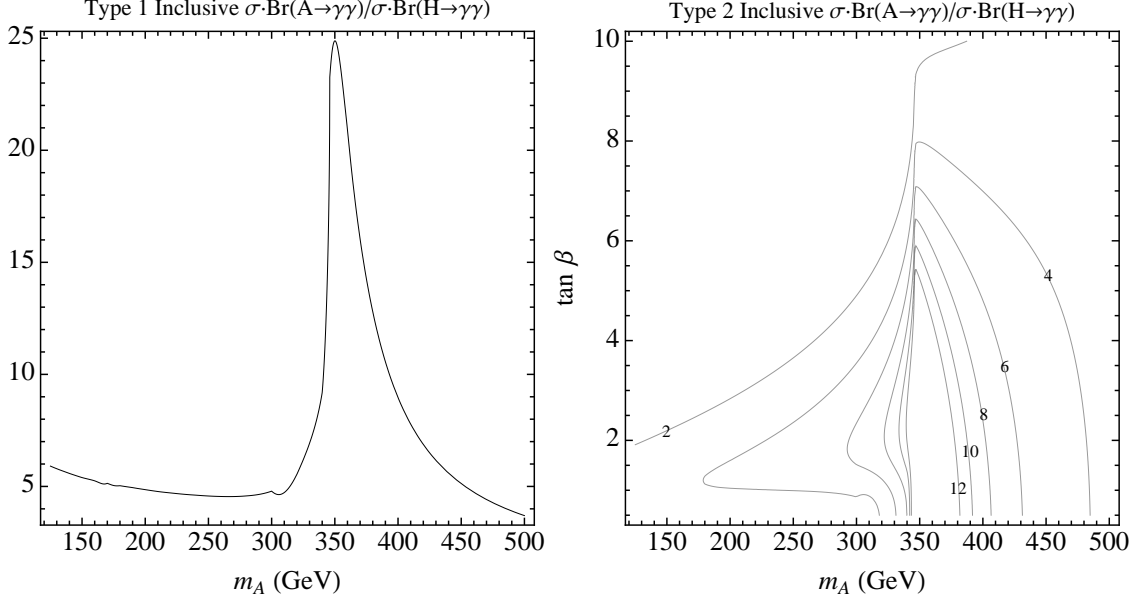


Figure 14. The inclusive $\sigma \cdot \text{Br}(A \rightarrow \gamma\gamma)/\sigma \cdot \text{Br}(H \rightarrow \gamma\gamma)$ for the pseudo-scalar and heavy scalar Higgs bosons in the $\sin^2(\beta - \alpha) = 1$ decoupling limit as a function of $m_A = m_H$ in Type 1 2HDM (left) and as a function of $m_A = m_H$ and $\tan\beta$ in Type 2 2HDM (right) assuming decays to Standard Model states only. The pseudo-scalar couples only to fermions, and in the decoupling limit the heavy scalar also couples only to fermions. Contours for Type 3 2HDM are similar to Type 1, and Type 4 2HDM to Type 2. The rapid change in the ratio for $m_A \gtrsim 2m_t$ is due to the top quark threshold.

In contrast the ratio $\sigma \cdot \text{Br}(H \rightarrow \gamma\gamma)/\sigma \cdot \text{Br}(A \rightarrow \gamma\gamma)$ in Type 2 2HDM, also shown in Fig. 14, does depend on $\tan\beta$ in the decoupling limit because the top and b -quark couplings have different $\tan\beta$ dependence. So in principle both A and H could be observed as two additional di-photon resonances beyond that of the SM-like Higgs, although the H resonance is generally somewhat weaker than the A resonance. The search for these two resonances over the full experimentally accessible mass range represents an important probe of the low $\tan\beta$ region of any of the 2HDMs. Observation of these two di-photon resonances would give accurate measures of the masses that could in turn yield additional information about the Higgs self couplings [26].

7 Conclusion

A variety of inclusive and exclusive standard Higgs search channels should be observable for a light SM-like Higgs boson with relatively low integrated luminosity at the LHC. These standard channels are likely to provide the first indications for a SM-like Higgs boson of any deviations of cross section times branching ratios from Standard Model expectations. In this paper we have focused on the standard channel signatures of CP and flavor conserving extended electroweak symmetry breaking sectors with two Higgs doublets. These models exhibit a variety of novel features which may be used to distinguish various types of 2HDM theories from the Standard Model Higgs and from each other in the event of discrepancies in certain channels.

Several features stand out. The combination of inclusive di-photon, VBF and Vh di-photon, and exclusive ditau $\sigma \cdot \text{Br}$ is often sufficient to differentiate different 2HDM types from each other and from

the Standard Model. If the exclusive di-photon $\sigma \cdot \text{Br}$ is significantly enhanced relative to the inclusive rate, this suggests theories in which all quarks couple to the same Higgs doublet. In contrast, if the inclusive and exclusive di-photon $\sigma \cdot \text{Br}$ are significantly enhanced this points to theories in which the up-type and down-type quarks couple to separate doublets. These inclusive and exclusive di-photon $\sigma \cdot \text{Br}$ may be largely verified by corresponding diboson $\sigma \cdot \text{Br}$, while exclusive ditau $\sigma \cdot \text{Br}$ resolve the leptonic couplings.

Various ratios of inclusive and exclusive channels may also be observed, enjoying reduced systematics relative to measurements of individual $\sigma \cdot \text{Br}$. The available inclusive ratios are not strongly sensitive to deviations from SM couplings in 2HDMs, in large part because of the parametric similarities in the hVV and $h\gamma\gamma$ couplings. However, exclusive ratios such as the ratio of VBF ditau and VBF diboson $\sigma \cdot \text{Br}$ are quite sensitive to deviations from SM couplings, and may vary sharply from the Standard Model prediction.

Intriguingly, the regions of 2HDM parameter space in which the light CP even neutral scalar h exhibits significant deviations from Standard Model Higgs signals also entail significant couplings of the heavier neutral scalars H and A to visible Standard Model states. Perhaps the most promising channels among these are $H \rightarrow VV$, and $H, A \rightarrow \gamma\gamma$, all of which enjoy considerable reach at the LHC. Notable discrepancies in the Standard Model signals of h can imply that decays of heavier scalars may be visible in standard Higgs channels, provided the scalars are not too heavy.

Finally, we note that the potential exclusive signatures of the MSSM Higgs are a subset of those presented here, as the MSSM is a Type II 2HDM with a specific set of coupling relations that reduce the number of free parameters. In particular, the angle α is fixed in terms of $\tan\beta$ and the Higgs masses. When $\tan\beta > 1$ this typically leads to an enhancement of the $\Gamma(h \rightarrow b\bar{b})$ partial width, making it difficult to enhance the inclusive and exclusive di-photon $\sigma \cdot \text{Br}$ in the MSSM without introducing additional degrees of freedom.

Acknowledgments

We thank Kfir Blum, Spencer Chang, Jared Evans, Jamison Galloway, and Can Kilic for useful conversations. This work was supported in part by DOE grant DE-FG02-96ER40959. NC gratefully acknowledges the support of the Institute for Advanced Study.

References

- [1] S. Chatrchyan *et al.* [CMS Collaboration], “Combined results of searches for the standard model Higgs boson in pp collisions at $\sqrt{s} = 7$ TeV,” *Phys. Lett. B* **710**, 26 (2012) [arXiv:1202.1488 [hep-ex]].
- [2] G. Aad *et al.* [ATLAS Collaboration], “Combined search for the Standard Model Higgs boson using up to 4.9 fb⁻¹ of pp collision data at $\sqrt{s} = 7$ TeV with the ATLAS detector at the LHC,” *Phys. Lett. B* **710**, 49 (2012) [arXiv:1202.1408 [hep-ex]].
- [3] D. Carmi, A. Falkowski, E. Kuflik and T. Volansky, “Interpreting LHC Higgs Results from Natural New Physics Perspective,” arXiv:1202.3144 [hep-ph].
A. Azatov, R. Contino and J. Galloway, “Model-Independent Bounds on a Light Higgs,” arXiv:1202.3415 [hep-ph].
J. R. Espinosa, C. Grojean, M. Muhlleitner and M. Trott, “Fingerprinting Higgs Suspects at the LHC,” arXiv:1202.3697 [hep-ph].

- A. Azatov, R. Contino, D. Del Re, J. Galloway, M. Grassi and S. Rahatlou, “Determining Higgs couplings with a model-independent analysis of $h \rightarrow \gamma\gamma$,” arXiv:1204.4817 [hep-ph].
- J. R. Espinosa, M. Muhlleitner, C. Grojean and M. Trott, “Probing for Invisible Higgs Decays with Global Fits,” arXiv:1205.6790 [hep-ph].
- A. Azatov, S. Chang, N. Craig and J. Galloway, “Early Higgs Hints for Non-Minimal Supersymmetry,” arXiv:1206.1058 [hep-ph].
- A. Azatov, R. Contino and J. Galloway, “Contextualizing the Higgs at the LHC,” arXiv:1206.3171 [hep-ph].
- D. Carmi, A. Falkowski, E. Kuflik and T. Volansky, “Interpreting the Higgs,” arXiv:1206.4201 [hep-ph].
- [4] M. Klute, R. Lafaye, T. Plehn, M. Rauch and D. Zerwas, “Measuring Higgs Couplings from LHC Data,” arXiv:1205.2699 [hep-ph].
- [5] R. S. Gupta, H. Rzehak and J. D. Wells, “How well do we need to measure Higgs boson couplings?,” arXiv:1206.3560 [hep-ph].
- [6] T. Plehn, D. L. Rainwater and D. Zeppenfeld, “Determining the structure of Higgs couplings at the LHC,” Phys. Rev. Lett. **88**, 051801 (2002) [hep-ph/0105325].
- [7] E. Contreras-Campana, N. Craig, R. Gray, C. Kilic, M. Park, S. Somalwar and S. Thomas, “Multi-Lepton Signals of the Higgs Boson,” JHEP **1204**, 112 (2012) [arXiv:1112.2298 [hep-ph]].
- [8] P. M. Ferreira, R. Santos, M. Sher and J. P. Silva, “Implications of the LHC two-photon signal for two-Higgs-doublet models,” arXiv:1112.3277 [hep-ph].
- A. Arhrib, C. -W. Chiang, D. K. Ghosh and R. Santos, “Two Higgs Doublet Model in light of the Standard Model $H \rightarrow \tau^+\tau^-$ search at the LHC,” Phys. Rev. D **85**, 115003 (2012) [arXiv:1112.5527 [hep-ph]].
- P. M. Ferreira, R. Santos, M. Sher and J. P. Silva, “Could the LHC two-photon signal correspond to the heavier scalar in two-Higgs-doublet models?,” Phys. Rev. D **85**, 035020 (2012) [arXiv:1201.0019 [hep-ph]].
- A. Arhrib, R. Benbrik and N. Gaur, “ $H \rightarrow \gamma\gamma$ in Inert Higgs Doublet Model,” Phys. Rev. D **85**, 095021 (2012) [arXiv:1201.2644 [hep-ph]].
- E. Gabrielli, B. Mele and M. Raidal, “Has a fermiophobic Higgs boson been detected at the LHC?,” arXiv:1202.1796 [hep-ph].
- K. Blum and R. T. D’Agnolo, “2 Higgs or not 2 Higgs,” arXiv:1202.2364 [hep-ph].
- D. Carmi, A. Falkowski, E. Kuflik and T. Volansky, “Interpreting LHC Higgs Results from Natural New Physics Perspective,” arXiv:1202.3144 [hep-ph].
- A. Barroso, P. M. Ferreira, R. Santos and J. P. Silva, “Probing the scalar-pseudoscalar mixing in the 125 GeV Higgs particle with current data,” arXiv:1205.4247 [hep-ph].
- A. Azatov, S. Chang, N. Craig and J. Galloway, “Early Higgs Hints for Non-Minimal Supersymmetry,” arXiv:1206.1058 [hep-ph].
- [9] S. Chatrchyan *et al.* [CMS Collaboration], “Search for the standard model Higgs boson decaying into two photons in pp collisions at $\sqrt{s}=7$ TeV,” arXiv:1202.1487 [hep-ex].
- [10] [ATLAS Collaboration], “Search for the Standard Model Higgs boson in the di-photon decay channel with 4.9 fb-1 of pp collisions at $\sqrt{s}=7$ TeV with ATLAS,” arXiv:1202.1414 [hep-ex].
- [11] S. Chatrchyan *et al.* [CMS Collaboration], “Search for the standard model Higgs boson in the decay channel H to ZZ to 4 leptons in pp collisions at $\sqrt{s} = 7$ TeV,” arXiv:1202.1997 [hep-ex].
- [12] [ATLAS Collaboration], “Search for the Standard Model Higgs boson in the decay channel $H \rightarrow ZZ(*) \rightarrow 4l$ with 4.8 fb-1 of pp collisions at $\sqrt{s}=7$ TeV with ATLAS,” arXiv:1202.1415 [hep-ex].
- [13] S. Chatrchyan *et al.* [CMS Collaboration], “Search for the standard model Higgs boson decaying to a W pair in the fully leptonic final state in pp collisions at $\sqrt{s} = 7$ TeV,” arXiv:1202.1489 [hep-ex].

- [14] S. Chatrchyan *et al.* [CMS Collaboration], “Search for neutral Higgs bosons decaying to tau pairs in pp collisions at $\sqrt{s}=7$ TeV,” arXiv:1202.4083 [hep-ex].
- [15] S. Chatrchyan *et al.* [CMS Collaboration], “Search for the standard model Higgs boson decaying to bottom quarks in pp collisions at $\sqrt{s}=7$ TeV,” arXiv:1202.4195 [hep-ex].
- [16] D. Zeppenfeld, R. Kinnunen, A. Nikitenko and E. Richter-Was, “Measuring Higgs boson couplings at the CERN LHC,” Phys. Rev. D **62**, 013009 (2000) [hep-ph/0002036].
- [17] M. Duhrssen, ”Prospects for the measurement of Higgs boson coupling parameters in the mass range from 110 - 190 GeV” ATL-PHYS-2003-030.
- [18] M. Duhrssen, S. Heinemeyer, H. Logan, D. Rainwater, G. Weiglein and D. Zeppenfeld, “Extracting Higgs boson couplings from CERN LHC data,” Phys. Rev. D **70**, 113009 (2004) [hep-ph/0406323].
- [19] C. Ruwedel, N. Wermes and M. Schumacher, “Prospects for the measurement of the structure of the coupling of a Higgs boson to weak gauge bosons in weak boson fusion with the ATLAS detector,” Eur. Phys. J. C **51**, 385 (2007).
- [20] R. Lafaye, T. Plehn, M. Rauch, D. Zerwas and M. Duhrssen, “Measuring the Higgs Sector,” JHEP **0908**, 009 (2009) [arXiv:0904.3866 [hep-ph]].
- [21] S. L. Glashow and S. Weinberg, “Natural Conservation Laws for Neutral Currents,” Phys. Rev. D **15**, 1958 (1977).
- [22] G. C. Branco, P. M. Ferreira, L. Lavoura, M. N. Rebelo, M. Sher and J. P. Silva, “Theory and phenomenology of two-Higgs-doublet models,” arXiv:1106.0034 [hep-ph].
- [23] M. Carena, S. Gori, N. R. Shah and C. E. M. Wagner, “A 125 GeV SM-like Higgs in the MSSM and the $\gamma\gamma$ rate,” JHEP **1203**, 014 (2012) [arXiv:1112.3336 [hep-ph]].
A. Arvanitaki and G. Villadoro, “A Non Standard Model Higgs at the LHC as a Sign of Naturalness,” JHEP **1202**, 144 (2012) [arXiv:1112.4835 [hep-ph]].
B. Batell, S. Gori and L. -T. Wang, “Exploring the Higgs Portal with 10/fb at the LHC,” arXiv:1112.5180 [hep-ph].
- [24] J. F. Gunion, H. E. Haber, G. L. Kane and S. Dawson, “The Higgs Hunter’s Guide,” Front. Phys. **80**, 1 (2000).
- [25] LHC Higgs Cross Section Working Group, S. Dittmaier, C. Mariotti, G. Passarino, and R. Tanaka (Eds.), *Handbook of LHC Higgs Cross Sections: 1. Inclusive Observables*, CERN-2011-002 (CERN, Geneva, 2011), arXiv:1101.0593 [hep-ph].
- [26] M. Dine, N. Seiberg and S. Thomas, “Higgs physics as a window beyond the MSSM (BMSSM),” Phys. Rev. D **76**, 095004 (2007) [arXiv:0707.0005 [hep-ph]].